

Contribution of meteorological input in calibrating a distributed hydrologic model in a watershed in the Tianshan Mountains, China

Gonghuan Fang · Jing Yang · Yaning Chen ·
Changchun Xu · Philippe De Maeyer

Received: 16 October 2014 / Accepted: 25 February 2015
© Springer-Verlag Berlin Heidelberg 2015

Abstract Water resources are essential to the ecosystem and social economy worldwide, especially in the desert and oasis of the Tarim River Basin, whose water originates largely from the Tianshan Mountains characterized by complicated hydrologic processes and scarce meteorological observations. In this study, distributed hydrologic model of SWAT (Soil and Water Assessment Tool) was applied to the Kaidu River Basin, a watershed in the Tianshan Mountains and one of the headwaters of the Tarim River. To quantify the contribution of meteorological input to model output, a sensitivity analysis approach (SDP method, State-Dependent Parameter method) was applied before and after the model was calibrated. The sensitivity analysis shows that meteorological input contributes up to 64 % of model uncertainty due to scarcity of observed meteorological data especially in the alpine region, and the groundwater flow is the most important hydrologic process in this watershed. Model calibration is

robust with Nash–Sutcliffe coefficients (“NS”s) and “ R^2 ”s over 0.80 for both the calibration period and the validation period where the length of the validation period is five times longer than the calibration period. The significance is obvious when compared to the simulation without considering the effect of spatial variation in meteorological input (NS = 0.80 and NS = 0.47 for “with lapse rates” and “without lapse rates”, respectively). Accurate meteorological input is of great importance to the distributed hydrological model, especially in the mountainous regions.

Keywords Meteorological input · Hydrologic modeling · Hydrologic process · Sensitivity analysis · Model calibration

Introduction

The Tarim River (Fig. 1), the longest inland river in China, is suffering from the ecological degradation, which is caused by over-consumption of water and its special hydrological conditions (Chen et al. 2011; Liu et al. 2011). It mainly originates from the Tianshan Mountains, runs through the oasis and finally disappears in the desert. With critical ecological problems such as the drying of river channel, weak water reproducible ability, deterioration of groundwater quality, degradation of natural vegetation and desertification in recent decades, water is even crucial in the Tarim River Basin (Wu 2012; Li et al. 2014). As one of its headwaters, the Kaidu River, provides 78 % water demand of the artificial oasis around the Bosten Lake with a population of 1.15 million (Chen et al. 2013). Therefore, the Kaidu River is crucial to the eco-environmental and economic development of the lower reaches of the Tarim River.

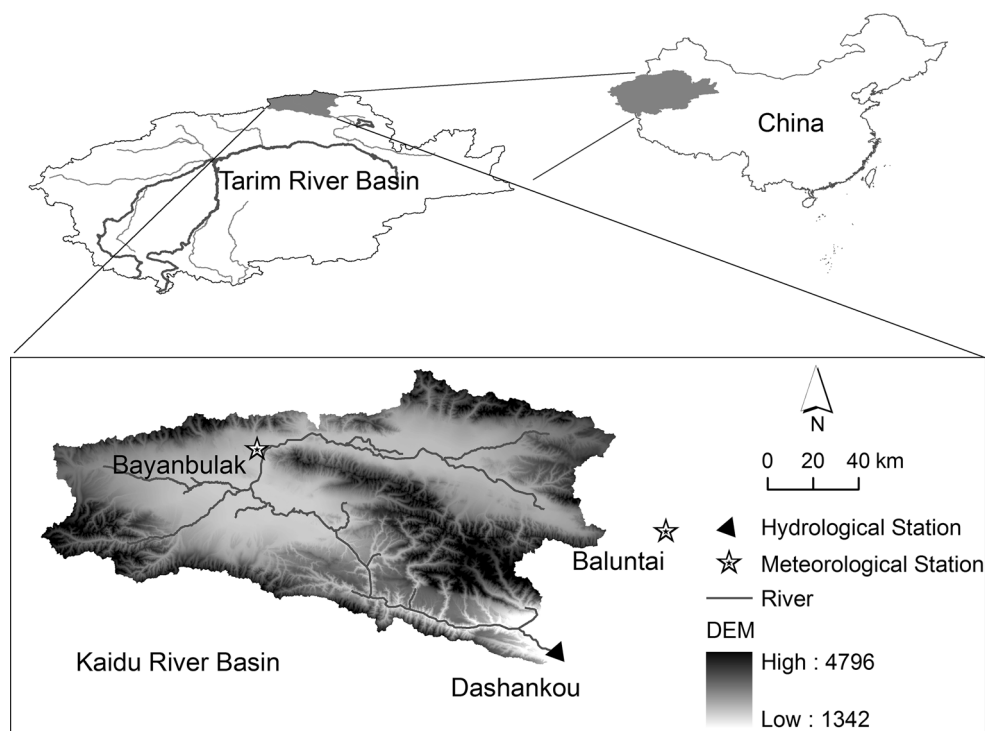
G. Fang · J. Yang (✉) · Y. Chen
State Key Laboratory of Desert and Oasis Ecology, Xinjiang
Institute of Ecology and Geography, Chinese Academy of
Sciences, 818 South Beijing Road, Urumqi 830011, Xinjiang,
China
e-mail: yangjing@ms.xjb.ac.cn

G. Fang
University of Chinese Academy of Sciences, Beijing 100049,
China

G. Fang · P. De Maeyer
Department of Geography, Ghent University, Gent 9000,
Belgium

C. Xu
Key Laboratory of Oasis Ecology, School of Resources and
Environmental Science, Xinjiang University, Xinjiang 830046,
China

Fig. 1 The location, topography and river system of the Kaidu River Basin



In spite of the importance of this watershed, there are few studies focusing on hydrological process due to the complicated topographic features and data scarcity (e.g., few meteorological data) in the alpine area and almost no study on the impact of meteorological input. Most studies either focus on flow forecast (e.g., Kalra et al. 2013; de la Paix et al. 2012), conducting a short period of flow simulation (e.g., Huang et al. 2010; Dou et al. 2011), or simulations with lumped models (e.g., Yang et al. 1987). As these studies are limited in understanding the watershed hydrology, distributed hydrologic modeling with a long-term simulation is appealing. Furthermore, as there is a data scarcity in meteorological input, which is very crucial to hydrologic modeling (Bobba et al. 1999; Gourley and Vieux 2005), it is necessary to study the impact of meteorological input. More generally, though it has been proven that meteorological input influences the hydrologic model a lot (e.g., Tavakoli and De Smedt 2013), to our best knowledge, few papers deal with how much this influence is and how much it affects model calibration. This is the major goal of this paper.

To achieve this goal, distributed hydrologic model of SWAT (Arnold et al. 1998) was applied to this watershed. To handle a large number of distributed parameters and understand the impact of meteorological input, a sensitivity analysis approach which combines the Morris method (Morris 1991) and the SDP method (Ratto et al. 2007) was conducted to understand dominant hydrologic processes and quantify the effect of meteorological inputs on model

calibration. The remaining is constructed as follows: Sect. 2 introduces the hydrologic model and study area; Sect. 3 describes the sensitivity analysis and calibration approaches; and then Sect. 4 gives results and discussion, followed by conclusions in Sect. 5.

Hydrologic model and study area

SWAT model

SWAT (Arnold et al. 1998), developed at the Agriculture Research Service of the United States Department of Agriculture, has been used for comprehensive modeling of the impacts of management practices and climate change on water and sediment yield and water quality at a watershed scale. It is a distributed hydrological model that runs on a daily step. To represent the spatial variability, a watershed is firstly divided into subbasins and each subbasin is then divided into hydrologic response units based on soil and landuse data. In SWAT, the simulation is based on water balance theory and runoff is predicted separately for each subbasin, which is illustrated in Fig. 2, and routed to obtain total runoff for the basin.

The climatic data required consists of daily precipitation, maximum/minimum air temperature, wind speed, relative humidity and solar radiation. SWAT uses elevation bands to represent the topographic effects on precipitation and temperature. Within each elevation band, the

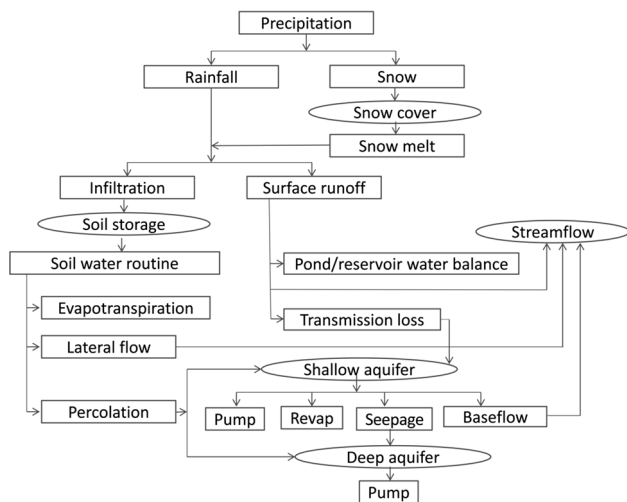


Fig. 2 Hydrologic flow chart of SWAT. Boxes donate different hydrological processes, ellipses different water storages and arrows water flow directions (Adapted from Arnold et al. 1998)

precipitation and temperature are estimated based on their lapse rates and elevation. For more details, refer to SWAT manuals (<http://www.brc.tamus.edu/>).

Study area and data collection

The Kaidu River Basin, with a drainage area of 18,634 km² above the Dashankou hydrological station, is located on the south slope of the Tianshan Mountains, Northwest China. The basin extends from 82°58' to 86°05'E, and from 42°14' to 43°21'N (Fig. 1). The altitude ranges from 1340 to 4796 m above sea level (asl) with an average elevation of 2995 m and an average slope of 23 %. This watershed has a complex topography including grassland, marsh, and surrounding mountainous alpine areas (Dou et al. 2011).

This watershed is characterized as temperate continental climate with alpine climate characteristic. The average annual temperature at the Bayanbulak meteorological station is -4.16 °C and annual precipitation is 287 mm, and generally precipitation falls as rain from May to September each year and as snow from October to April of the next year. The average daily flow at the Dashankou hydrological station is around 110 m³ s⁻¹ (equivalent to 185 mm runoff), ranging from 15 to 973 m³ s⁻¹. Watershed hydrology is driven by snowmelt in spring and rainfall/snowmelt in summer. Data used in this study include:

Meteorological data and hydrologic data

Daily meteorological data of two stations are from China Meteorological Data Sharing Service System (<http://cdc.cma.gov.cn/>) from 1980 to 2010. One station is the Bayanbulak Station (2458 m asl), which lies in the valley

of mountainous regions in the watershed, and the other is the Baluntai Station (1740 m asl), which is near the study region. Discharge data at the Dashankou hydrologic station are from Xinjiang Tarim River Basin Management Bureau. Available data include daily discharge from 1980 to 2002 and monthly discharge from 2003 to 2010.

Digital elevation model (DEM)

The 90 m DEM is from the Shuttle Radar Topography Mission (NASA, <http://www2.jpl.nasa.gov/srtm/>). DEM forms the basis for determining the drainage area, flow direction, basin boundary, etc.

Soil data

Soil map, with a scale of 1:1000,000 is from Xinjiang Institute of Ecology and Geography, Chinese Academy of Sciences. The spatial distribution of soil is shown in Fig. 3 (top) and the corresponding proportions are listed in Table 1 (left). Soil texture, soil depth and other information of each soil type were from Agricultural bureau and soil survey office of Xinjiang (1996).

Landuse data

Landuse map with a scale of 1:100,000 is from the Environmental and Ecological Science Data Center for West China. Spatial distribution of landuse type is shown in Fig. 3 (bottom) and relevant proportions are listed in Table 1 (right).

Model setup and initial parameter selection

After pre-processing these data in ArcSWAT (swat.tamu.edu/software/arcswat/), the SWAT model (version 2009) was set up with the following options: (1) Elevation band and lapse rate were used to represent the topographic effects on precipitation and temperature in the mountainous region; (2) Penman–Monteith method (Monteith 1965) was utilized to calculate potential evapotranspiration; (3) The degree-day approach, which is generally deemed as an effective method to handle snow pack and snowmelt in data scarce mountains (Li and Williams 2008), was used to model snowmelt; (4) Variable storage routing method (Williams 1969) was used for river routing.

Model parameters related to flow simulation were initially selected based on literature review and SWAT user manual (Arnold et al. 2011). When calibrating distributed model parameters, a factor which denotes a way to change a group of parameters was used to avoid confusion with model parameters (e.g., factor *r_CN2* is to relatively change all distributed parameters *CN2*, and *v_Tlaps* is to

Fig. 3 The spatial distribution of soil (*top*) and landuse (*bottom*) in the Kaidu River Basin

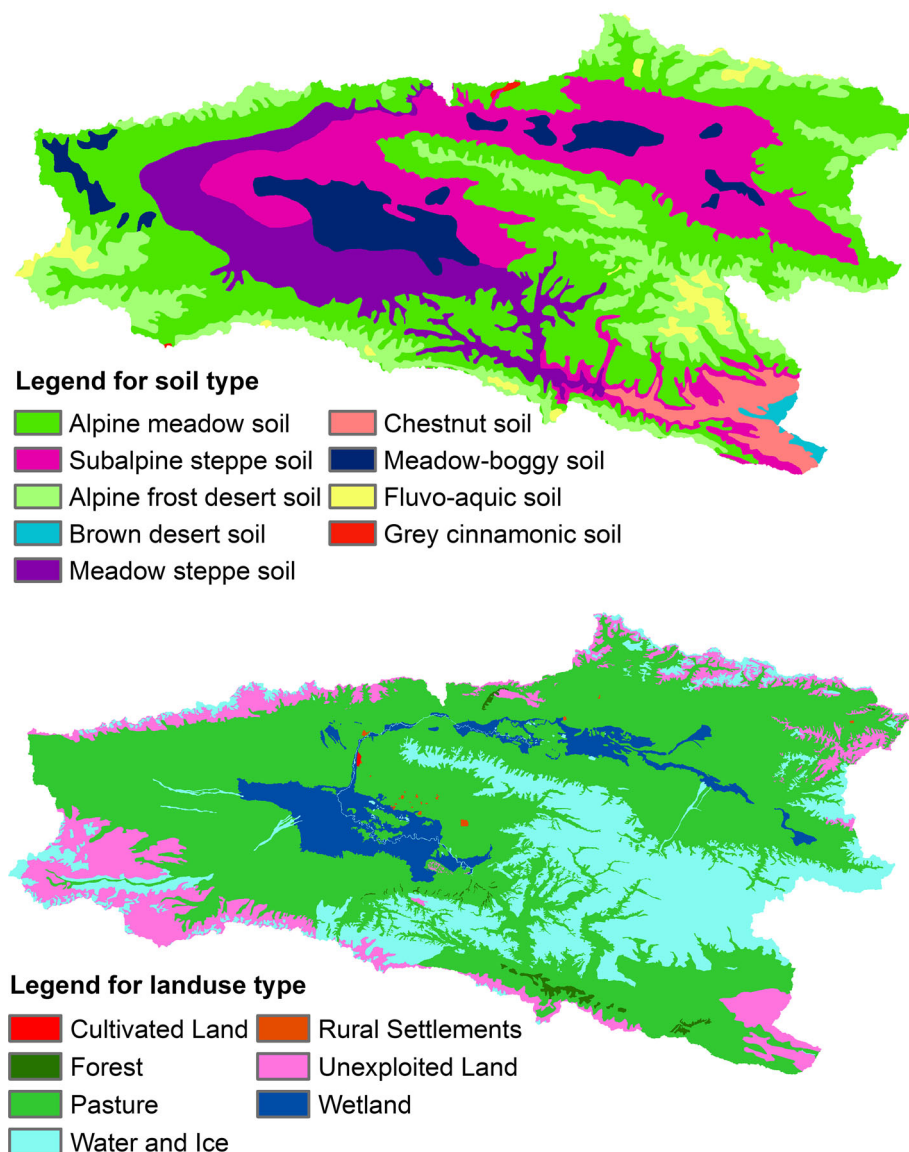


Table 1 Proportions of the soil types (left) and the landuse types (right) in the watershed

Soil type	Proportion (%)	Landuse type	Proportion (%)
Alpine meadow soil	38.0	Pasture	61.3
Subalpine steppe soil	21.4	Water and ice	20.9
Alpine frost desert soil	16.0	Unexploited land	11.0
Brown desert soil	12.4	Wetland	6.1
Meadow steppe soil	7.0	Forest	0.5
Chestnut soil	2.6	Rural Settlements	0.1
Meadow-boggy soil	1.9	Cultivated land	0.1
Fluvo-aquic soils	0.4		
Gray cinnamonic soil	0.1		

replace all parameters T_{laps}), as proposed in Yang et al. (2007). Table 2 lists these factors along with their meanings of their underlying parameters and ranges, among

which $v_{T_{laps}}$ and $v_{P_{laps}}$, the values of the lapse rates of temperature and precipitation, are two factors to measure the topographical variation of meteorological input.

Table 2 Selected factors and their initial values and ranges for sensitivity analysis, and their estimated values

No.	Factor ^a	Range ^b	Underlying SWAT parameter	Initial value	Estimated value
1	<i>v__Tlaps</i>	[-10, 0]	<i>Tlaps</i> : Temperature lapse rate (°C km ⁻¹)	0	-9.23
2	<i>v__Alpha_bf</i>	[0, 1]	<i>Alpha_bf</i> : Baseflow alpha factor	0.048	0.94
3	<i>v__Plaps</i>	[100, 200]	<i>Plaps</i> : Precipitation lapse rate (mm km ⁻¹)	0	165.00
4	<i>v__Gwqmn</i>	[0, 1000]	<i>Gwqmn</i> : Threshold water level in shallow aquifer for baseflow (mm)	00	72.00
5	<i>r__Sol_k</i>	[-0.5, 2]	<i>Sol_kl</i> : Saturated hydraulic conductivity (mm h ⁻¹)	0	0.87
6	<i>v__Gw_delay</i>	[0, 500]	<i>Gw_delay</i> : Groundwater delay time (day)	31	340.60
7	<i>v__Esco</i>	[0, 1]	<i>Esco</i> : Soil evaporation compensation factor (-)	0.95	0.36
8	<i>r__Slsubbsn</i>	[-0.3, 0.3]	<i>Slsubbsn</i> : Average slope length (m)	0	0.15
9	<i>v__Ch_k2</i>	[0, 500]	<i>Ch_k2</i> : Effective hydraulic conductivity in main channel alluvium (mm h ⁻¹)	0	253.10
10	<i>r__Sol_awc</i>	[-0.5, 0.5]	<i>Sol_awc</i> : Available water capacity of the soil layer (-)	0	-0.21
11	<i>r__CN2</i>	[-0.15, 0.15]	<i>CN2</i> : SCS runoff curve number for moisture condition	0	0.04
12	<i>v__Smfmx</i>	[-0, 10]	<i>Smfmx</i> : Snowmelt factor on June 21 (mm °C ⁻¹ d ⁻¹)	4.5	7.71
13	<i>r__Sol_z</i>	[-0.5, 0.5]	<i>Sol_z</i> : Depth from soil surface to bottom of layer (mm)	0	-
14	<i>v__Gw_revap</i>	[-0.02, 0.2]	<i>Gw_revap</i> : Groundwater “revap” coefficient	1.0	-
15	<i>v__Surlag</i>	[0, 24]	<i>Surlag</i> : Surface runoff lag time (day)	4	-
16	<i>v__Revapmn</i>	[0, 500]	<i>Revapmn</i> : Threshold depth of water in shallow aquifer for revap (mm)	1.0	-
17	<i>r__Slope</i>	[-0.1, 0.1]	<i>Slope</i> : Average slope steepness (-)	0	-
18	<i>v__Ch_k1</i>	[0, 300]	<i>Ch_k1</i> : Effective hydraulic conductivity in tributary channel alluvium (mm h ⁻¹)	0	-
19	<i>v__Smfmn</i>	[0, 10]	<i>Smfmn</i> : Snowmelt factor on Dec. 21 (mm °C ⁻¹ d ⁻¹)	4.5	-
20	<i>v__Epc</i>	[0, 1]	<i>Epc</i> : Plant uptake compensation factor	1.0	-
21	<i>v__Ch_n2</i>	[0, 0.3]	<i>Ch_n2</i> : Manning’s “n” for main channel (-)	0.18	-
22	<i>r__OV_N</i>	[-0.5, 0.5]	<i>OV_N</i> : Manning’s “n” for overland flow (-)	0.15	-
23	<i>r__Sol_alb</i>	[-0.2, 0.2]	<i>Sol_alb</i> : Moist soil albedo (-)	0	-
24	<i>v__Sftmp</i>	[-1, 1]	<i>Sftmp</i> : Snowfall temperature (°C)	1.0	-
25	<i>v__Smtmp</i>	[-1, 1]	<i>Smtmp</i> : Snow melt base temperature(°C)	0.5	-

^a Here, ‘v__’ or ‘r__’ means a replacement or a relative change to the initial parameter values

^b The ranges for the factors are based on literature data (e.g., the range of *v__Plaps* is from Zhou 1999) and SWAT user’s manual (Arnold et al. 2011)

This work studied the contribution of meteorological input through these two factors. To investigate the impact of spatial variation of meteorological input, another simulation was set up without these two lapse rates (i.e., excluding *v__Tlaps* and *v__Plaps*), and refer this to “without lapse rates” and the previous to “with lapse rates”, respectively.

A warm-up period is normally used to eliminate the influence of initial state variables (e.g., soil moisture, groundwater storage, etc.) on simulation, and the longer the warm-up period, the less effect initial state variables will have on the simulation (Yang et al. 2012). In this study, a seven-year period (1979–1985) was used for model warm-up after some tests. To calibrate the model, the split sample procedure was used: daily data from 1986 to 1989 were used for model calibration, and daily data from 1990 to 2002 (first validation period) and monthly data from 2003 to 2010 (second validation period) were used to test the

model performance. Both calibration and validation contain dry and wet years, and longer validation period was used to show the robustness of the calibrated model.

Methodology

Sensitivity analysis

Sensitivity analyses are valuable tools for identifying important model parameters (in this case is “factors”). In this study, a sensitivity analysis approach combining the Morris method (Morris 1991) and the SDP method (Ratto et al. 2007) was applied to screen out unimportant factors and identify the most important ones. Its applications range from simple conceptual model (e.g., HYMOD in Yang 2011) to physical and distributed models (e.g. TOPMODEL in Ratto et al. 2007; Wetspa in Yang et al. 2012;

MOBIDIC in Yang et al. 2014), and it has been proven to be effective and efficient. Firstly the Morris method was used to screen out insensitive hydrological factors and thus to reduce the number of factors for next sensitivity analysis. In the second step, the SDP was implemented to quantitatively compute the main effect and first-order interactions between these reduced factors.

Morris method

The Morris method is a qualitative method to measure factor sensitivity and factor interaction or nonlinearity. For a n -dimensional random variable $X = (x_1, \dots, x_i, \dots, x_n)$ at its j th sample $(x_{1j}, \dots, x_{ij}, \dots, x_{nj})$, the local sensitivity measure (elementary effect) d_{ij} for x_i at j th sample is computed based on OAT (One-At-a-Time) as follows:

$$d_{ij} = \frac{f(x_{1j}, \dots, x_{ij} + \Delta, \dots, x_{nj}) - f(x_{1j}, \dots, x_{ij}, \dots, x_{nj})}{\Delta}, \quad i = 1, 2, \dots, n; j = 1, 2, \dots, m \tag{1}$$

where $f(\cdot)$ is the model output (or relevant objective function), X are model factors with x_i normalized to $[0,1]$ to eliminate the scale effect, and $\Delta = \frac{p}{2(p-1)}$ is the predefined increment and normally p takes the value within the range of $[4,10]$ (Saltelli 1999) and in this study p was set to 10 meaning $\Delta = 5/9$. Local sensitivity measures of each input factor are estimated by randomly sampling in the factor space, by which a finite distribution of the local sensitivity measures obtained. For example, for basic sample size m , one can obtain a group of elementary effects d_{ij} ($i = 1, \dots, m$) for factor x_i . From these values, two statistics are obtained: one is the mean of absolute values of the elementary effects (μ^*), which measures the factor sensitivity (e.g., for x_i , $\mu_i^* = \sum_{j=1}^m |d_{ij}|/m$), and the other is the standard deviation of the elementary effects (σ), which measures the degree of factor interaction or nonlinearity (e.g.,

$$\text{for } x_i, \quad \sigma_i = \sqrt{\sum_{j=1}^m \left(d_{ij} - \frac{\sum_{j=1}^m d_{ij}}{m} \right)^2} / (m - 1).$$

The higher μ^* is, the more important the factor is to model output, and the higher (σ), the more interactions are with other factors or more nonlinear to the model output. Totally, the Morris method needs $m^*(n + 1)$ model runs to estimate these two sensitivity indices for each factor, and normally $m = 50$ is sufficient (Yang et al. 2012).

State-dependent parameter method (SDP)

For independent input factors, SDP method is based on the idea of the decomposition of variance of model output Y to factors X :

$$V = \sum_i V_i + \sum_i \sum_{j>i} V_{ij} + \dots + V_{1,2,\dots,n} \tag{2}$$

where,

$$V_i = V(E(Y|X_i))$$

$$V_{ij} = V(E(Y|X_i, X_j)) - V_i - V_j$$

and so on. Herein, $V(\cdot)$ and $E(\cdot)$ denote variance and expectation operators, V is the total variance, and V_i and V_{ij} are total variance and partial variances of the i th factor. Normalize these variances with V , the following sensitivity indices can be obtained:

$$S_i = \frac{V_i}{V}, 1 \leq i \leq n \tag{3}$$

$$S_{ij} = \frac{V_{ij}}{V}, 1 \leq i < j \leq n \tag{4}$$

$$S_{Ti} = S_i + \sum_j S_{ij} + \sum_j \sum_k S_{ijk} + \dots + S_{1,2,\dots,n}, 1 \leq i \leq n \tag{5}$$

where S_i is the main effect, which represents the average achieved reduction of output variance when factor X_i is fixed, S_{ij} is the second-order interaction between X_i and X_j , and S_{Ti} is the total effect representing the average output variance when X_i stays unfixed. In practice, S_i is used to measure the average variance in the output that can be reduced when X_i is fixed and S_{Ti} is used to measure the average variance in the output remains when X_i stays unfixed (Tarantola et al. 2002).

The SDP method is based on recursive filtering and smoothing estimation and can estimate these main effects (S_i) and first-order interactions (S_{ij}) based on its approximation to second-order ANOVA regression model. And ‘‘quasi-total effect’’, $S_{Di} = S_i + \sum_j S_{ij}$, is used to approximate S_{Ti} when R^2 of second-order ANOVA is high enough (e.g., larger than 0.80).

Model calibration and evaluation

To calibrate the distributed hydrological model, SCE-UA method (Duan et al. 1992) was used. This algorithm has been proven to be consistent, effective, and efficient in locating the globally optimal model parameters of a hydrologic model (Gupta et al. 1999).

The objective function for calibration is Nash–Sutcliffe coefficient (NS) (Nash and Sutcliffe 1970):

$$NS = 1 - \frac{\sum_{i=1}^n (Y_i^{obs} - Y_i^{sim})^2}{\sum_{i=1}^n (Y_i^{obs} - Y^{mean})^2} \tag{6}$$

where Y_i^{obs} and Y_i^{sim} are the i th observed and simulated flows, Y^{mean} is the mean of observed data, and n is the number of observations. NS donates how well the

simulation matches the observation. NS ranges between $-\infty$ and 1.0, with $NS = 1$ meaning a perfect fit. The higher this value, the more reliable the model is.

To evaluate model performance, in addition to NS, percent bias (PBIAS) and coefficient of determination (R^2) were also used. PBIAS is computed as:

$$PBIAS = \frac{\sum_{i=1}^n (Y_i^{sim} - Y_i^{obs})}{\sum_{i=1}^n (Y_i^{obs})} \quad (7)$$

PBIAS measures the average deviation of the simulated data from their observed counterparts. Positive values indicate an overestimation of the observation, while negative values indicate an underestimation. The smaller of $|PBIAS|$, the smaller deviation of the simulation. Generally, $|PBIAS| < 10\%$ shows good modeling. R^2 describes the degree of collinearity between simulated and measured data. Normally $NS > 0.50$, $|PBIAS| < 25\%$ and $R^2 > 0.6$ are taken as the criteria of satisfactory modeling of the river discharge, and model performance can be evaluated as excellent if $NS > 0.75$ and $|PBIAS| < 10\%$ (Moriassi et al. 2007).

In this study, the simulation “with lapse rates” and simulation “without lapse rates” were analyzed separately following the same procedure. Firstly, the Morris method was applied to initially selected factors (Table 2) to screen out the unimportant factors, and then the sensitivities of the sensitive ones were quantified by the SDP method. Secondly, the calibration was applied to the important factors, followed by another sensitivity analysis with the SDP method. The contribution of the meteorological input was analyzed based on the sensitivity and calibration results, and the comparison between the simulation “with lapse rates” and simulation “without lapse rates”.

Results and discussion

In this section, we mainly presented and discussed the result of the simulation “with lapse rates”, and the result of simulation “without lapse rates” was only for the comparison purpose. Hereafter, results and discussion are based on the simulation “with lapse rates” unless otherwise specified.

Sensitivity analysis

With $m = 50$, the Morris method took 1300 model runs. Figure 4 shows the sensitivity result for each factor based on the Morris method, where μ^* represents its sensitivity and σ its interaction with other factors or nonlinearity of the factor. These twenty-five factors were grouped into three classes visually based on their “ μ^* ”: extremely sensitive, medially sensitive and insensitive. v_Tlaps ,

v_Alpha_bf and v_Plaps are the extremely sensitive factors with strong nonlinearity in the meanwhile. v_Tlaps and v_Plaps influence the temperature and precipitation input in each elevation band, and have intense impact on water yield and water balance. v_Alpha_bf , representing the baseflow recession constant, describes the response of groundwater to recharge change and is an important factor that influences groundwater flow. The medium sensitivity class includes 7 factors: v_Gwqmn and v_Gw_delay are factors related to groundwater flow and groundwater–stream water interactions; v_Ch_k2 , r_Sol_k and r_Sol_awc dominate the infiltration of surface water into groundwater; v_Esco , with its underlying parameter *Esco* being the compensation factor of soil evaporation, controls the actual evapotranspiration; r_Ssubsn is factor indicating the changes of average slope length. Factors at the bottom left of Fig. 4 including r_CN2 and v_Smfmx are insensitive. Note that r_CN2 is not sensitive in this study while it was extremely sensitive in many previous studies (e.g., Van Griensven et al. 2006; Saha et al. 2014). This might be attributed to the hydrological characteristics of the Kaidu River Basin: it has a large area of wetland (1137 km²) and flatland (37 % of the study area with a slope under 8.7 %). The high proportion of wetland and flatland resulted in the low sensitivity of r_CN2 as identified by Schmalz et al. (2009). All snowmelt-related factors, e.g., v_Smfmx , v_Sftmp , v_Smtmp , are not sensitive, which indicates that snow process is not so important in the Kaidu River Basin. This is corroborated with an analysis of average monthly precipitation allocation: the precipitation from October to March (winter season) only consists of 9 and 4 % of the yearly precipitation at Bayanbulak and Balutai, respectively.

After excluding insensitive factors identified by the Morris method, the SDP method was applied to estimate the main effect (S_i) and first-order interaction (S_{ij}) of the sensitive factors. To ensure that all potential sensitive

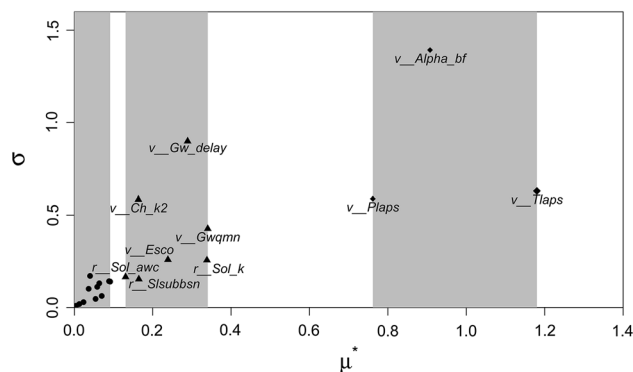


Fig. 4 Factor sensitivity based on the Morris method (diamond denotes extremely sensitive, triangle medially sensitive, and closed circle insensitive)

factors are quantified, another two factors, i.e., r_CN2 and v_Smfmx , the most sensitive ones in the insensitive group, were also included. Therefore, 12 factors were analyzed using SDP method. It took 600 model runs and the R^2 of the second-order ANOVA model is 93.0 %, which means it explains over 90 % of the model uncertainty (i.e., variation of NS). The result is shown in Table 3. The most sensitive factor is v_Tlaps , followed by v_Plaps and v_Alpha_bf . Other factors are not so sensitive for both S_i and S_{Di} . v_Tlaps and v_Plaps control the driving force (i.e., precipitation and temperature), and the main effect of these two factors is 64.0 % (i.e. sum of main effects of v_Tlaps and v_Plaps , and their first-order interaction), contributing to over half of the model uncertainty. v_Alpha_bf influences the groundwater flow and its main effect is 13 %. This suggests that fixing of these three factors (e.g. through calibration) leads to over 77 % reduction of model uncertainty. This result is the same as that based on the Morris method. It is worth noting that the low sensitivity indices of other factors do not mean that they are not sensitive but that their contribution to the model output is not as significant as these three factors.

Model calibration and evaluation

Calibration was then carried out on these twelve factors using SCE-UA method. With daily NS = 0.80 during the calibration period, the optimal values are given in Table 2. The calibrated v_Plaps is 165 mm km⁻¹, which is very close to other studies in this region (e.g., 162 mm km⁻¹ in Lin 1985; 156.4 mm km⁻¹ in Zhao et al. 2011). v_Tlaps is -9.23 °C km⁻¹, within the range of the study of Chen (2012) (i.e., from -11.8 to -7.3 °C km⁻¹) based on temperature data from several stations in the south slope of Tianshan Mountains. This temperature lapse rate, which is close to the dry adiabatic lapse rate (-9.8 °C km⁻¹), is related to the characteristics of our study region, i.e., a mountainous watershed located in the arid area with low pressure, low humidity and high wind speed (e.g., Blandford et al. 2008). The mean pressure and relative humidity are 0.828×10^5 Pa and 42 % at Baluntai Station, and 0.758×10^5 Pa and 69 % at Bayanbulak Station. Besides, there are over 12 % of days with wind speed higher than 5 m s⁻¹ (strong wind) and 38 % of days higher than 3 m s⁻¹ (moderate to strong wind) at Bayanbulak Station.

As discussed above, the hydrologic response is dominated by the meteorological input. By fixing two factors v_Tlaps and v_Plaps to their optimal values, another SDP application was performed to the remaining ten factors to study the important hydrologic processes without the influence of meteorological input. As it turns out, the most sensitive factors are v_Alpha_bf ($S_i = 0.57$) and v_Gw_delay ($S_i = 0.29$), less sensitive factors are

Table 3 The main effect (S_i), quasi-total effect (S_{Di}) and the first-order interaction (S_{ij} , the triangular matrix on the right) of factors as percentage based on the SDP method. The values are given with only one decimal place

Factor	S_i	S_{Di}	S_{ij}	v_Tlaps	v_Alpha_bf	v_Plaps	v_Gwqmn	r_Sol_k	v_Gw_delay	v_Esco	$r_Ssubbsn$	v_Ch_k2	r_Sol_awc	r_CN2	v_Smfmx
v_Tlaps	37.8	41.5													
v_Alpha_bf	13.0	13.3	0.2												
v_Plaps	24.6	27.5	1.6	0.0											
v_Gwqmn	1.6	2.0	0.3	0.0	0.0										
r_Sol_k	7.3	9.0	1.1	0.0	0.0	0.1									
v_Gw_delay	0.3	1.2	0.2	0.0	0.0	0.7	0.0	0.0							
v_Esco	0.9	1.2	0.2	0.0	0.0	0.0	0.0	0.1	0.0						
$r_Ssubbsn$	0.9	1.3	0.1	0.0	0.0	0.2	0.0	0.1	0.0	0.0					
v_Ch_k2	0.0	0.1	0.0	0.1	0.0	0.0	0.0	0.0	0.0	0.0	0.0				
r_Sol_awc	0.3	0.3	0.0	0.0	0.0	0.0	0.0	0.0	0.0	0.0	0.0	0.0			
r_CN2	0.0	0.0	0.0	0.0	0.0	0.0	0.0	0.0	0.0	0.0	0.0	0.0	0.0		
v_Smfmx	0.9	1.0	0.0	0.0	0.0	0.1	0.0	0.0	0.0	0.0	0.0	0.0	0.0	0.0	
R^2	87.6	93.0													

Table 4 Model performances for the calibration and validation periods

Statistics	NS	PBIAS (%)	R ²
“With lapse rates”			
Calibration period 1986–1989 (daily data)	0.80	0.01	0.80
First validation period 1990–2002 (daily data)	0.81	2.94	0.81
Second validation period 2003–2010 (monthly data)	0.86	1.31	0.87
“Without lapse rates”			
Calibration period 1986–1989 (daily data)	0.47	–30.22	0.66
First validation period 1990–2002 (daily data)	0.49	–32.22	0.71
Second validation period 2003–2010 (monthly data)	0.35	–36.51	0.80

r_Sol_k ($S_i = 0.02$) and v_Smfmx ($S_i = 0.02$) and other factors are only sensitive through the interaction with these factors. Factors related to groundwater process (i.e. v_Alpha_bf , v_Gw_delay) account for more than 80 % of the model uncertainty (sum of main effects of these two factors and first-order interactions between them). Although by the Morris method, v_Smfmx is an insensitive factor, it is a relatively sensitive one by the SDP method when fixing v_Tlaps and v_Plaps . It is indicative that the dominant hydrological process is the groundwater flow, and then the snowmelt flow and evapotranspiration. To verify the importance of groundwater, a baseflow separation was done to the observed discharge using the digital filter technique (Arnold et al. 1995), which shows that groundwater contributes to 72–86 % of the total flow (or runoff). The high percentage of groundwater might be due to the large flat valley area between steep mountains, i.e., large area of wetland and flatland as is indicated in Sect. 4.1.

Table 4 and Fig. 5 show agreement between the simulated and observed flow series. As indicated by the statistics in Table 4, the model performs well for both the calibration period (1986–1989) and validation periods (first validation period 1990–2002 and second validation period 2003–2010), in spite of the length of the validation period is five times longer than the calibration period. The “NS”s, “PBIAS”s, “R²”s are 0.80, 0.01 %, 0.80 for the calibration period, 0.81, 2.94 %, 0.81 for the first validation period, and 0.86, 1.31 %, 0.87 for the second validation period. These “NS”s, “PBIAS”s, and “R²”s are within the excellent range proposed by Moriasi et al. (2007).

The statistics above are corroborated by Fig. 5. In Fig. 5, the simulated flow matches the observation very well except for some peaks in summer seasons in 1987, 1999 and 2002. This might be due to the glacier melt in summer which is not accounted for in this model. Generally, the model can simulate the flow response to the rainfall and snowmelt. Notice there is a fluctuation in the baseflow since 1992 when the Dashankou hydropower station (4 km above the Dashankou hydrological station)

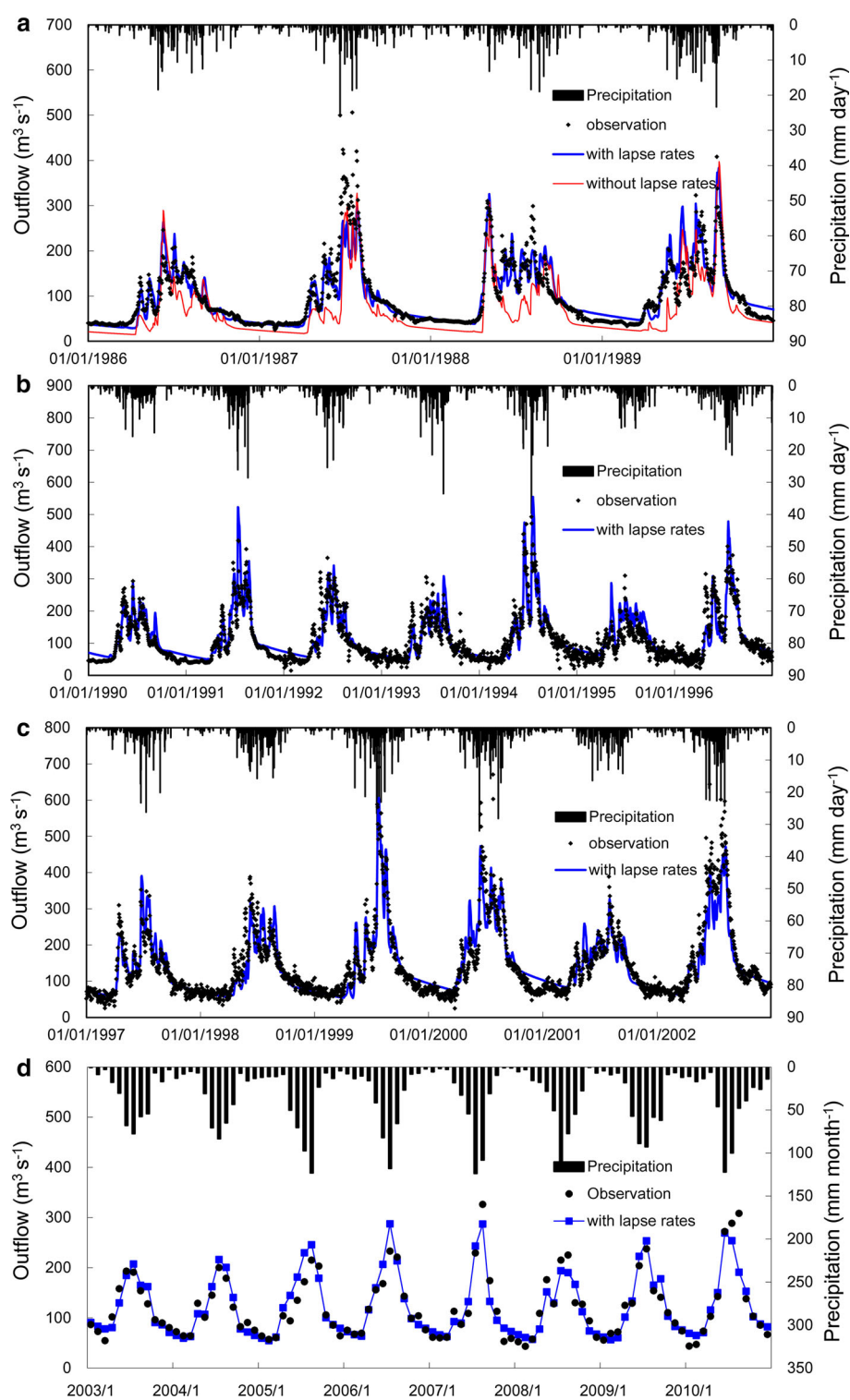
started to operate. However, this hydropower station does not seem to have too much effect on the daily outflow.

To demonstrate the effect of the meteorological input, the results of the simulation “without lapse rates” are also shown in Table 4 and Fig. 5a. Compared to simulation “with lapse rates”, simulation “without lapse rates” was unable to capture most of the discharges in the Kaidu River Basin, with NS equals to 0.47 for the calibration period, 0.49 for the first validation period and 0.35 for the second validation period. Snowmelts in spring (e.g., in 1986, 1987 and 1989) were underestimated, peaks in summer (e.g., in 1988) were not captured, and baseflow was extremely underestimated. For “without lapse rates”, the underestimation of the baseflow is mainly related to over-simplification of spatial distribution of precipitation and temperature. As a result, this leads to less average annual precipitation (252 mm) and higher average temperature (5.1 °C) than these of “with lapse rate” whose average annual precipitation is 378 mm and average temperature is –1.9 °C. When driving the hydrologic model, it will cause less precipitation input and higher evapotranspiration, and this leads to less groundwater recharge, and eventually less groundwater discharge. Figure 6 shows how different the spatial variation of annual average precipitation using precipitation lapse rate (Fig. 6a) from the one without precipitation lapse rate (Fig. 6b). This shows the importance of spatial variation of meteorological input in calibrating a distributed hydrological model and confirms the conclusion that high quality of distributed rainfall data contributes to good hydrological model performance (Tavakoli and De Smedt 2013; Lee et al. 2013).

Conclusions

This paper implemented a combined sensitivity analysis approach to the application of SWAT in the Kaidu River Basin to investigate the contribution of meteorological input in calibrating distributed hydrologic model. The following conclusions can be drawn:

Fig. 5 Observed and simulated outflow series at the Dashankou hydrological station during the calibration period (**a** daily streamflow) and the validation period (**b, c** daily streamflow and **d** monthly streamflow)



1. Our model is an effective tool to simulate the hydrologic processes. Simulated daily flow series are in agreement with the observed ones, with “NS”s and “ R^2 ”s over 0.80 and IPBIASI < 3 % for both calibration period and validation period. This calibration is

robust and tested by the validation period whose length is five times longer than the calibration period.
 2. Sensitivity analysis shows v_Tlaps and v_Plaps are the two most important factors with main effects of 64.0 %. This indicates the model uncertainty largely

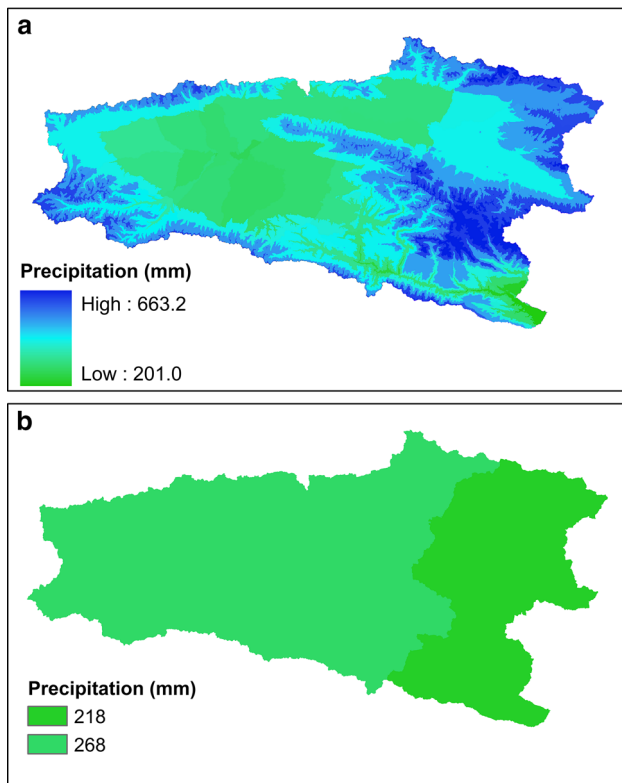


Fig. 6 Spatial distribution of annual mean precipitation for simulations with lapse rates (a) and without lapse rates (b)

results from the meteorological inputs due to the scarcity of observed meteorological data, especially in the alpine regions.

- Groundwater flow is the most important hydrologic process in this watershed. Fixing v_Tlaps and v_Plaps to their optimal values, factors related to groundwater process account for over 80 % of the model uncertainty, which is consistent with the result of baseflow separation using digital filter technique.
- Compared to the simulation “without lapse rates”, the simulation “with lapse rates” shows significant improvement on daily flows, especially in baseflow simulation (groundwater discharge), which suggests high spatial resolution meteorological data (e.g., satellite data) should be used for hydrologic modeling in this region.

Acknowledgments The research was supported by the “Thousand Youth Talents” Plan (Xinjiang Project: Y371051), the National Natural Science Foundation of China (41471030) and the Foundation of State Key Laboratory of Desert and Oasis Ecology (Y371163).

Conflict of interest The authors declare that they have no conflict of interest.

Ethical approval This article does not contain any studies with human participants or animals performed by any of the authors.

Informed consent Informed consent was obtained from all individual participants included in the study.

References

Agricultural bureau and soil survey office of Xinjiang (1996) Xinjiang soil. Science Press, Beijing

Arnold JG, Allen P, Muttiah R, Bernhardt G (1995) Automated base flow separation and recession analysis techniques. *Ground Water* 33:1010–1018

Arnold JG, Srinivasan R, Muttiah RS, Williams J (1998) Large area hydrologic modeling and assessment part I: model development. *J Am Water Resour As* 34:73–89

Arnold JG, Kiniry J, Srinivasan R, Williams J, Haney E, Neitsch S (2011) Soil and Water Assessment Tool input/output file documentation, version 2009

Blandford TR, Humes KS, Harshburger BJ, Moore BC, Walden VP, Ye H (2008) Seasonal and synoptic variations in near-surface air temperature lapse rates in a mountainous basin. *J Appl Meteorol Clim* 47:249–261

Bobba AG, Jeffries DS, Singh VP (1999) Sensitivity of hydrological variables in the Northeast Pond River watershed, Newfoundland, Canada, due to atmospheric change. *Water Resour Manag* 3:171–188

Chen X (2012) Hydrological model of inland river basin in arid land. China Environmental Science Press, Beijing

Chen Z, Chen Y, Li W, Chen Y (2011) Changes of runoff consumption and its human influence intensity in the mainstream of Tarim river. *Acta Geogr Sin* 66:89–98

Chen Y, Du Q, Chen Y (2013) Sustainable water use in the Bosten Lake Basin. Science Press, Beijing

De la Paix MJ, Li LH, Ge JW, de Dieu HJ, Theoneste N (2012) Analysis of snowmelt model for flood forecast for water in arid zone: case of Tarim River in northwest China. *Environ Earth Sci* 66:1423–1429

Dou Y, Chen X, Bao A, Li L (2011) The simulation of snowmelt runoff in the ungauged Kaidu River Basin of TianShan Mountains, China. *Environ Earth Sci* 62:1039–1045

Duan Q, Sorooshian S, Gupta V (1992) Effective and efficient global optimization for conceptual rainfall-runoff models. *Water Resour Res* 28:1015–1031

Gourley JJ, Vieux BE (2005) A method for evaluating the accuracy of quantitative precipitation estimates from a hydrologic modeling perspective. *J Hydrometeorol* 6:115–133

Gupta HV, Sorooshian S, Yapo PO (1999) Status of automatic calibration for hydrologic models: comparison with multilevel expert calibration. *J Hydroaul Eng* 4:135–143

Huang Y, Chen X, Li Y, Willems P, Liu T (2010) Integrated modeling system for water resources management of Tarim River Basin. *Environ Eng Sci* 27:255–269

Kalra A, Li L, Li X, Ahmad S (2013) Improving streamflow forecast lead time using oceanic-atmospheric oscillations for Kaidu River Basin, Xinjiang, China. *J Hydrol Eng* 18:1031–1040

Lee G, Yu W, Jung K (2013) Catchment-scale soil erosion and sediment yield simulation using a spatially distributed erosion model. *Environ Earth Sci* 70:33–47

Li X, Williams MW (2008) Snowmelt runoff modelling in an arid mountain watershed, Tarim Basin, China. *Hydrol Process* 22:3931–3940

Li Q, Zhou JL, Zhou YZ, Bai CY, Tao HF, Jia RL, Ji YY, Yang GY (2014) Variation of groundwater hydrochemical characteristics in the plain area of the Tarim Basin, Xinjiang Region, China. *Environ Earth Sci* 72:4249–4263

- Lin R (1985) Characteristics on the vertical distribution of precipitation and runoff in the south slope of the Tianshan Mountain. *Hydrology* 2:28–33
- Liu T, Willems P, Pan XL, Bao AM, Chen X, Veroustraete F, Dong QH (2011) Climate change impact on water resource extremes in a headwater region of the Tarim basin in China. *Hydrol Earth Syst Sci* 15:3511–3527
- Monteith JL (1965) Evaporation and environment. *Symp Soc Exp Biol* 19:205–234
- Moriasi DN, Arnold JG, Van Liew MW, Bingner RL, Harmel RD, Veith TL (2007) Model evaluation guidelines for systematic quantification of accuracy in watershed simulations. *T Asabe* 50:885–900
- Morris MD (1991) Factorial sampling plans for preliminary computational experiments. *Technometrics* 33:161–174
- Nash JE, Sutcliffe J (1970) River flow forecasting through conceptual models part I—A discussion of principles. *J Hydrol* 10:282–290
- Ratto M, Young PC, Romanowicz R, Pappenberger F, Saltelli A, Pagano A (2007) Uncertainty, sensitivity analysis and the role of data based mechanistic modeling in hydrology. *Hydrol Earth Syst Sci* 11:1249–1266
- Saha P, Zeleke K, Hafeez M (2014) Streamflow modeling in a fluctuant climate using SWAT: Yass River catchment in south eastern Australia. *Environ Earth Sci* 71:5241–5254
- Saltelli A (1999) Sensitivity analysis: could better methods be used? *J Geophys Res* 104:3789–3793
- Schmalz B, Fohrer N (2009) Comparing model sensitivities of different landscapes using the ecohydrological SWAT model. *Adv Geosci* 21:91–98
- Tarantola S, Giglioli N, Jesinghaus J, Saltelli A (2002) Can global sensitivity analysis steer the implementation of models for environmental assessments and decision-making? *Stoch Environ Res Risk Assess* 16:63–76
- Tavakoli M, De Smedt F (2013) Validation of soil moisture simulation with a distributed hydrologic model (WetSpa). *Environ Earth Sci* 69:739–747
- Van Griensven A, Meixner T, Grunwald S, Bishop T, Diluzio M, Srinivasan R (2006) A global sensitivity analysis tool for the parameters of multi-variable catchment models. *J Hydrol* 324:10–23
- Williams J (1969) Flood routing with variable travel time or variable storage coefficients. *Trans ASAE* 12:100–103
- Wu J (2012) Evaluation of the water resource reproducible ability on Tarim River Basin in south of Xinjiang, northwest China. *Environ Earth Sci* 66:1731–1737
- Yang J (2011) Convergence and uncertainty analyses in Monte-Carlo based sensitivity analysis. *Environ Modell Softw* 26:444–457
- Yang X, Jiang H, Huang C (1987) An applied study on the snowmelt type of Xinanjiang Watershed Model at the Kaidu River Basin. *J August 1st Agri Collage* 4:82–90
- Yang J, Reichert P, Abbaspour KC (2007) Bayesian uncertainty analysis in distributed hydrologic modeling: a case study in the Thur River basin (Switzerland). *Water Resour Res* 43:W10401
- Yang J, Liu Y, Yang W, Chen Y (2012) Multi-objective sensitivity analysis of a fully distributed hydrologic model WetSpa. *Water Resour Manag* 26:109–128
- Yang J, Castelli F, Chen Y (2014) Multiobjective sensitivity analysis and optimization of distributed hydrologic model MOBIDIC. *Hydrol Earth Syst Sci* 18:4101–4112
- Zhao C, Shi F, Sheng Y, Li J, Zhao Z, Han M, Yilibula Y (2011) Regional differentiation characteristics of precipitation changing with altitude in Xinjiang region in recent 50 years. *J Glaciol Geocryol* 6:1203–1213
- Zhou Y (1999) Xinjiang river hydrology and water resources. Xinjiang Science and Technology Press, Urumqi